A novel method for observing hip fracture during simulated sideways fall impact

E. K. Bliven[1,2], P. Guy[1,3], B. Helgason[4], and P. A. Cripton[1,2]
[1] Orthopaedic and Injury Biomechanics Group; [2] School of Biomedical Engineering; [3] Department of Orthopaedics
University of British Columbia
Vancouver, British Columbia, Canada
[4]Institute for Biomechanics, ETH-Zürich, Zürich, Switzerland

ABSTRACT

Hip fracture is a devastating injury associated with high rates of morbidity and mortality. Understanding the biomechanics of how these fractures occur is essential for the advancement of successful prevention strategies. Bone surfaces are usually not visible during impact tests of biofidelic specimens (with soft tissue surrogate), prohibiting proper visualization of fracture occurrence. Our research aims to develop and evaluate the suitability of a high-speed x-ray system as a tool for visualizing hip fracture, throughout the volume of the hip, during a realistic sideways fall impact. Previous work in our lab focused on the development of a pendulum fall simulator shown to successfully produce clinically relevant hip fracture patterns in inertia-driven impacts. In the present study, we supplemented this experimental set-up with a custom high-speed x-ray system consisting of an x-ray source, image intensifier, and high-speed video camera. Proof-of-concept methods included the optimization of the novel system by identifying parameters such as configuration, x-ray exposure factors, resolution, and capture rate. The feasibility of capturing fracture was tested with pilot fall tests using a surrogate femur-pelvis construct. Later trials investigated the potential for tracking metal beads and an orthopedic screw implanted in the proximal femur. We were able successfully integrate the novel system as well as capture fracture propagation and other behavior. Metal beads could be tracked to displacements below 0.1 mm. The results of this pilot work demonstrate the ability to observe hip fracture using the high-speed x-ray system with the previously developed fall simulator. The presented tool is theorized to offer more robust capabilities than current imaging techniques to observe bone mechanics during impact tests. Obtaining such data could be key to understanding and ultimately preventing hip fractures, particularly when an implant is present.

INTRODUCTION

Hip fracture is a traumatic and prevalent injury with worldwide incidence expected to reach 4.5 million annually by 2050 (Cooper et al., 2011). It is associated with high rates of morbidity and mortality: one in four patients dies within a year of injury (Haleem et al, 2008), (U.S. Congress, 1994). Despite being a relatively common occurrence, a fall from standing height can be particularly dangerous for vulnerable populations such as the elderly, and is the most common way for hip fracture to occur (Parkkari et al, 1999). Understanding the biomechanics of how these fractures occur is essential for the advancement of successful prevention strategies.

Several methods have been pursued to induce hip fracture experimentally in a setting that accurately mimics real-world occurrence of the injury. It is imperative that simulating the mechanism of hip fracture occur in as biofidelic a manner as possible, which requires including factors affecting the impact force delivered to the greater trochanter of the femur. Beyond variables such as subject mass and height, factors affecting force on the femur extend to the non-linear stiffness of the pelvis (Laing et al, 2010) and soft tissue thickness over the greater trochanter (Bouxsein et al., 2007). Both of these are accounted for in a test set-up previously developed in our lab to simulate a sideways fall (Fleps et al., 2018). The fall simulator consists of a pendulum impactor that guides cadaveric femur-pelvis specimens in an inertia-driven fall onto a force plate, as can be seen in Figure 1. Per this method, specimens are encased in a subject-specific mold of ballistic gel to mimic the compressive properties of soft tissues over the greater trochanter.

Visualizing the occurrence of hip fracture is relatively straightforward in less biofidelic test set-ups that apply force directly to the femur, which permit the use of high-speed video cameras to record skeletal surface phenomena (de Bakker et al., 2009). However, high-speed video collection is inadequate for the observation of hip fracture in specimens containing soft tissue surrogate. The presence of (usually opaque) soft tissue between the bony surface of the femur and recording equipment prevents accurate capture of this critical visual data without reliance on the extrapolation from soft tissue marker data or the like. Furthermore, the behavior of femur-implanted devices or materials during impact remain relatively unknown when relying on conventional imaging methods. Despite the moderate incidence (Della Rocca et al., 2011) and mortality (Bhattacharyya et al., 2007) associated with periprosthetic fracture, the relative motion of bone-implant constructs upon impact has not been widely studied in the biomechanics field.

Application of electromagnetic radiation via x-ray technology is a common non-invasive way of identifying hip fracture in patients. In experimental biomechanics settings, x-ray has been combined with high-speed video recording to capture phenomena such as brain motion during impact (Whyte et al., 2019), joint kinematics (Thorhauer et al., 2020), and compressive vertebral fractures (Diotalevi et al., 2020). However, utilizing high speed x-ray in an orthopedic trauma setting seems to be relatively uninvestigated, outside of a few studies (distal radius fracture in a fall (Gutowski et al., 2015) and impact of the mandible (Craig et al., 2008)). Approaches to date using x-ray to image femoral fracture in real-time have only been carried out on small, sub-organ level bone samples (Ma et al., 2020) or applied loading very slowly (Martelli et al., 2018). To the authors' knowledge, high speed x-ray capture of hip fracture in a realistic simulated fall scenario has not yet been pursued.

There remains a need for a method to observe hip fracture in biofidelic specimens as it occurs under realistic experimental impact conditions. Our goal in this pilot study was to evaluate the suitability of the high-speed x-ray system as a tool for visualizing hip fracture during a realistic sideways fall impact. This was pursued by addressing the following three aims: 1) identify optimal exposure factors and camera parameters for imaging bone through soft tissue surrogate, 2) establish system configuration to assess physical compatibility of the x-ray system and the fall simulator, and 3) investigate the feasibility of tracking metal beads and an orthopedic implant during fracture. Overall, this work aimed to demonstrate proof-of-concept feasibility of using the presented system to capture high-speed x-ray data of hip fracture as it occurs in a realistic impact.

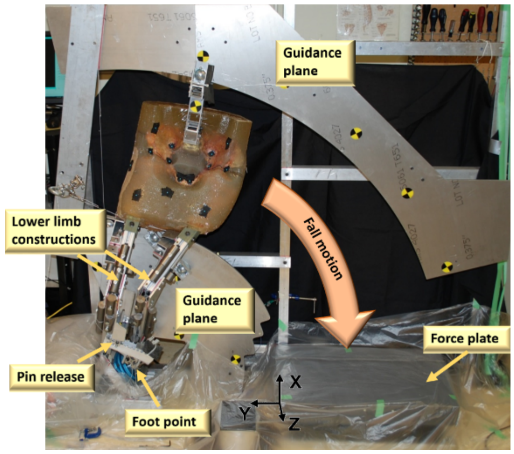

Figure 1: Experimental set-up simulating a sideways fall (from Fleps et al., 2018).

METHODS

The custom high-speed x-ray system used for all tests in this study consisted of an x-ray source (MXR-160/20, Comet AG, Switzerland) and image intensifier. A Phantom v12.1 high-speed camera (Vision Research Inc, Wayne, NJ) was mounted in the image intensifier and recorded the output window with settings such as recording rate, exposure, and resolution adjusted in the corresponding camera software. X-ray exposure factors were controlled using a microprocessor-based control panel set in fluoroscopy mode (MP1, Gulmay Ltd., Surrey, UK). Video files were post-processed using VirtualDub software (open-source, Avery Lee) for frame extraction and manipulation and ImageJ (National Institutes of Health, Bethesda, MD) to convert pixel values using an object of known distance.

Table 1. Specimen details per study phase

Phase	Imaging Mode	Specimen	Soft tissue surrogate	Orthopedic implant
1	Static	Porcine vertebra	✓	✗
2	Dynamic	Artificial femur (notched)	✗	✗
3	Dynamic	Artificial femur	✗	✓

This work was carried out in three phases of pilot tests, each with different experimental set-ups and specimens (Table 1). These phases were staged to subsequently address individual sub-aims of the overall goal of this study, which is to evaluate the feasibility of using high speed x-ray to capture hip fracture in a simulated sideways fall. The methods specific to each phase are outlined in sections below, primarily by way of repeated trials conducted and iteratively modulated using n=1 specimen per phase.

Phase 1: Static capture through soft tissue surrogate

Preliminary methods involved identifying parameters (exposure factors and camera settings) necessary to image bone through soft tissue surrogate with the x-ray system. Per the fall simulator methods, specimens are to be encased in 20 weight % ballistic gel cast in a subject-specific mould shape (Fleps et al., 2018). The proposed use of the x-ray system with this set-up requires capturing fracture through the anterior-posterior soft tissue thickness at the hip joint, which could be up to 90 mm in a larger specimen (measured from the surface of the proximal femur to the anterior surface of the gel.) We incorporated a factor of safety of ~1.5 in designing the specimen mold for this proof-of-concept test, with a thickness of 140 mm between the specimen surface and gel surface.

A porcine vertebra was embedded in a rectangular mold of ballistic gel. The specimen was placed in the gantry of the system at approximately 17 cm from the x-ray source and 11 cm from the image intensifier in the system's original configuration. The thickest part of the gel was oriented towards the image intensifier to account for potential posterior scatter after passing through the specimen. A series of static images was taken while the following parameters were iteratively adjusted: set-up orientation (distance between the source and image intensifier, specimen location between them, system alignment), x-ray exposure factors (emitted voltage (kV) and current (mA)), and high-speed camera settings (aperture, focus, resolution, and exposure). Per this system, setting exposure factors independently in manual fluoroscopy mode is subject to a machine safety limit of 640 W power.

Phase 2: Dynamic capture of hip fracture

Integrating the x-ray system into the fall simulator required moving and modifying the configuration so that the radiation field was centered at our region of interest: where the greater trochanter of the falling specimen impacts the force plate. The dimensions of the x-ray source in particular require that it be rotated 90° from its upright position and safe operation in this position was pre-emptively verified with the manufacturers of the x-ray source and cooling system. A series of pilot drops were conducted after x-ray images paired with positioning adjustments demonstrated a feasible configuration, shown in Figure 2.

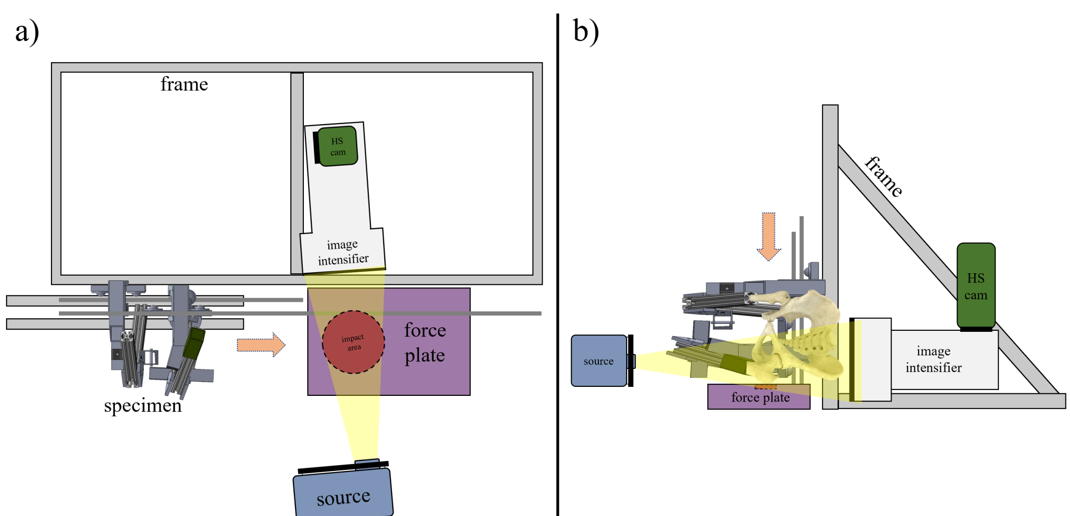

Figure 2: Final x-ray system configuration in the fall simulator, shown a) pre-fall from an overhead view, and b) post-fall from the side.

Each pilot drop was conducted with the same re-used surrogate pelvis and embedded contralateral femur, both artificial 4th generation Sawbones models (Pacific Research Company, Vashon Island, USA) made of polyurethane foam and epoxy composites. The ipsilateral and impacting side of the construct was always a left foam cortical Sawbones femur, embedded in 50 mm of bone cement at a distance 175 mm distal to the most lateral point of the greater trochanter. Specimens were subjected to a simulated sideways fall using the impactor and associated methods presented in Fleps' work (Fleps et al., 2018). The feasibility of incorporating the x-ray system into this set-up was then tested by conducting repeated drops with iterative adjustments (such as increasing fall energy and notching of the femoral neck) until specimen fracture occurred.

Phase 3: Tracking of orthopedic implant and metal beads

This phase continued the simulated fall tests using the pendulum impactor, with the additional measurement of impact force from a modified six-axis force plate (FP4000-15, Bertec Corporation, Columbus, OH) recording data at 10,000 Hz. Synchronization of the force transducer and high-speed camera was achieved using an electrical contact trigger. The pelvis-femur construct was prepared, aligned and embedded as described in Phase 2. A 6.5mm Ø cannulated cancellous screw with a 5mm Ø shaft (Depuy Synthes, USA) was implanted in a left Sawbones femur center-center along the femoral neck axis (Figure 3). The screw was implanted deep enough to ensure that the screwhead was unexposed and not making direct contact with the impact surface. The anterior surface of the specimen was seeded with four 3-mm spherical steel beads adhered in shallow pockets drilled into the cortical foam. Similar to the methods in Phase 2, simulated fall tests were conducted until fracture occurred. The beads and implant were tracked over the course of the fall using XMALab software, an open-source package for marker-based analysis of x-ray data (Knörlein et al., 2016).

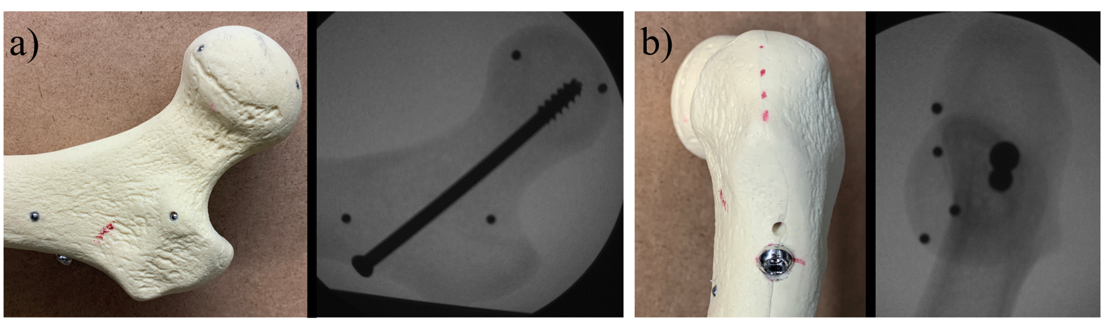

Figure 3: Images and radiographs of Phase 3 specimen in a) anterior-posterior, and b) medial-lateral views.

RESULTS

Phase 1: Static capture through soft tissue surrogate

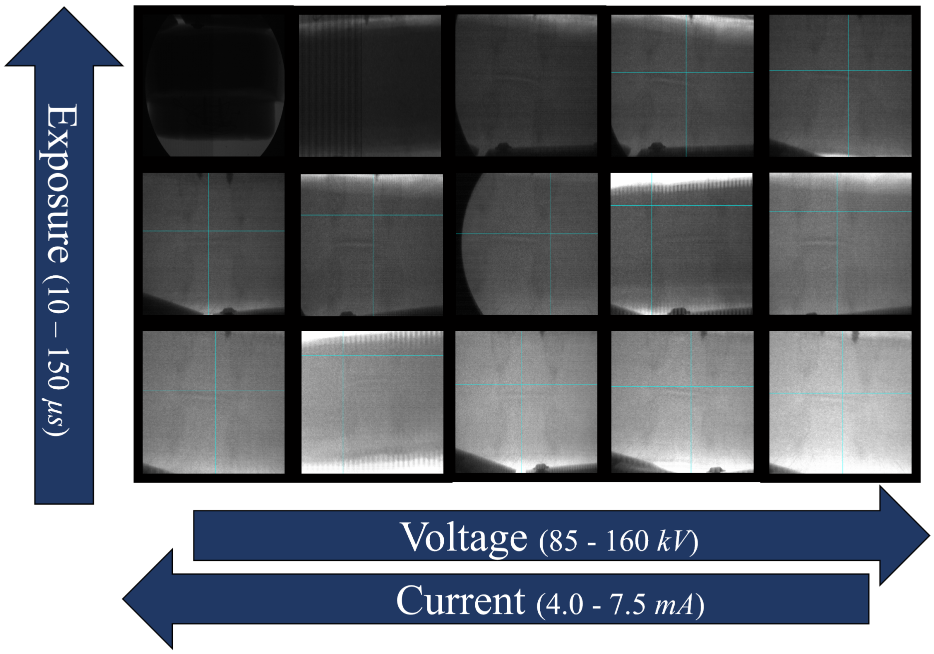

Figure 4: Matrix showing static radiographs of a porcine vertebra representing various applied parameters. Arrows indicate direction that range increases.

A grid of representative radiographs obtained from varying the x-ray exposure factors and camera exposure within their allowable ranges can be seen in Figure 4. Iterative adjustments revealed suitable visibility of the porcine vertebra at values in the range of 64-160 kV and 4-10mA, with a camera exposure between 10-50μs. Vertebra visibility was improved by positioning the specimen mould closer to the image intensifier within the aligned system components.

Phase 2: Dynamic capture of hip fracture

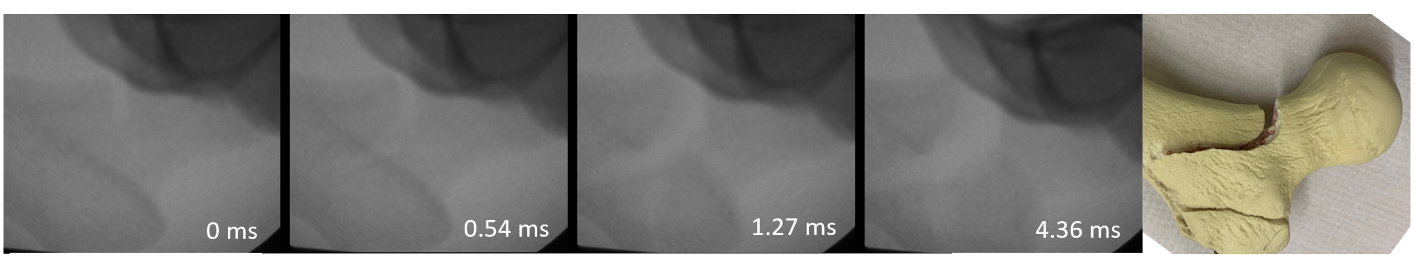

Figure 5: X-ray video frames showing fracture propagation in a sideways fall impact.

Impact of the surrogate femur onto the force plate was successfully captured using the high-speed x-ray system during the first simulated fall tests. However, fracture did not occur, with the femur specimen only exhibiting elastic bending of the femoral neck. After 5 kg of lead shot was added to the pelvic inlet of the specimen to increase fall energy, fracture was still not observed in a subsequent fall test. Specimen fracture occurred in the following test, after a small notch was cut in the inferior basicervical region of the femoral neck. Propagation of a multifragmentary pertrochanteric fracture was captured with the high-speed x-ray system. Initiating at the notch, the fracture was observed to traverse laterally across the femur within a span of 1.3 ms (Figure 5). The exposure factors were set for this phase of testing at 160 kV and 4 mA, and the video camera at an exposure of 20 μs with a collection rate of 11,000 fps.

Phase 3: Tracking of orthopedic implant and metal beads

The exposure factors used for these tests were at 64 kV and 10 mA, with an exposure of 30 μs and video camera collection rate of 8,900 fps. Initial simulated fall tests of the implanted and seeded femur did not result in fracture until the addition of 2.24 kg to the falling specimen. The first and primary fracture resulting from this drop propagated superolaterally across the femur over a span of 2.1 ms, during which the femur was unloaded from the peak recorded force of 1,563 N (Figure 6). Post-fracture visual inspection of the specimen revealed that the fracture path passed through the hole created in cortical bone to implant the screw. The fracture did not appear to intersect any of the indentations made for the inserted metal beads.

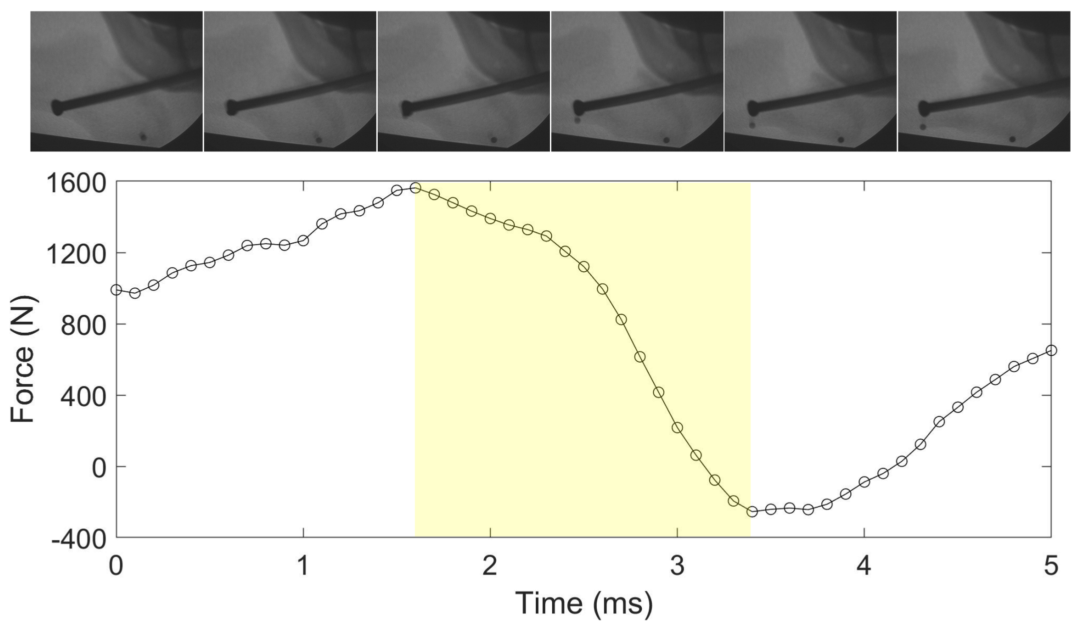

Figure 6: Force over time plotted between the maximum and minimum loads recorded during a sideways fall impact. X-ray stills show fracture occurring during the 2.1 ms window in the yellow shaded region.

Initial drops of the implanted specimen (sans fracture) were analyzed in XMALab to track 2D motion of the screw and metal beads (Figure 7) in a plane oriented perpendicular to the x-ray beam and roughly parallel to the anterior surface of the femoral shaft. This analysis included x-ray frames over a 12 ms period, during which free fall and subsequent impact on the force plate occurred. Tracking feasibility was verified and changes in bead position of less than

0.1 mm between x-ray frames were able to be detected. The tracked entities were shown to travel vertically in free fall at a speed of 2.9 m/s. The most superior bead exhibited larger displacements during impact than both the screwhead and inferior bead.

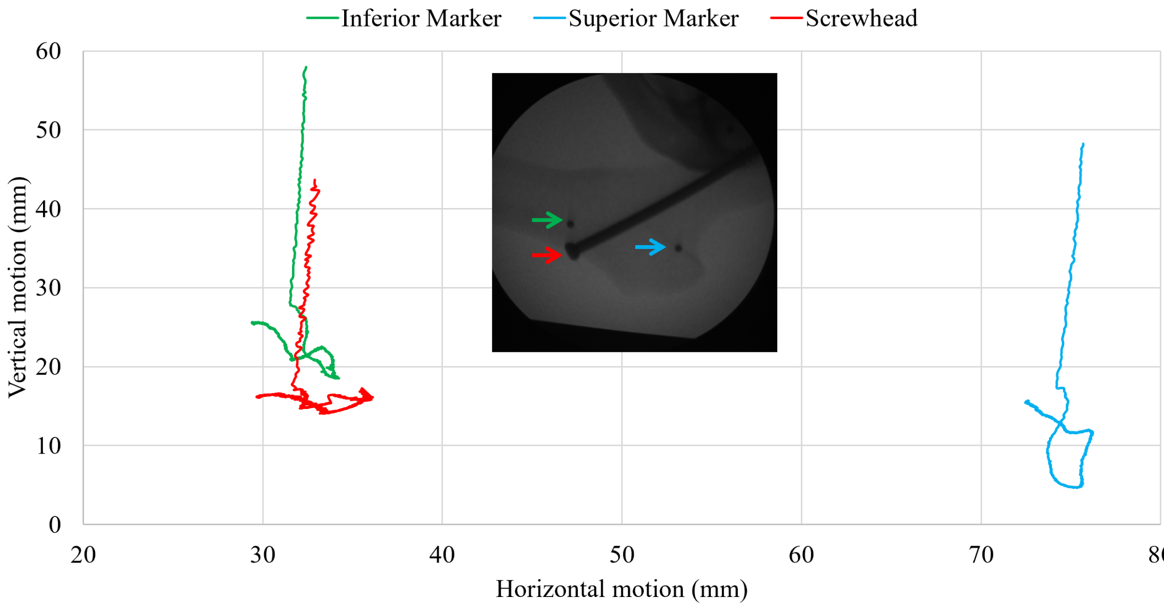

Figure 7: Marker and screwhead motion over 12 ms of a sideways fall and impact (no fracture).

DISCUSSION

The aim of this study was to evaluate the suitability of a novel method for capturing hip fracture in a sideways fall using high-speed x-ray. We sought to achieve this through a phased approach: by identifying system parameters necessary to visualize bone through relevantly dimensioned soft tissue surrogate, confirming physical compatibility of the x-ray system and fall simulator, and capturing fracture and metal bead motion during a simulated fall and impact. Each phase was pursued to address the primary obstacles anticipated in the development and verification of this imaging method. The presented work successfully demonstrates proof-of-concept feasibility of capturing hip fracture in a simulated fall with the described high-speed x-ray system.

Varying x-ray exposure factors, camera settings, and specimen-equipment positioning revealed parameter ranges suitable for imaging bone through thick soft tissue surrogate. Higher x-ray voltage values (kV) were deemed most important for improving contrast and visualizing bone. The nature of this work and use of cadaveric specimens allows for higher values to be used than what is clinically safe and acceptable. Improved resolution by positioning the specimen closer to the image intensifier was expected, as such a configuration reduces scatter after radiation passes through the medium and before it reaches the intensifier input window.

Physical integration of the high- speed x-ray components within the fall simulator set-up proved to be feasible after the configuration was adjusted iteratively, checking field of view with x-ray images. We were able to capture a multi-stage fracture propagating across the surrogate femur throughout the impact, with mechanical phenomena discernable in sub-millisecond time steps. The induced fracture was observed to initiate at the notch cut in the inferior femoral neck. This behavior is not surprising, as a stress concentration was essentially introduced in the region of the bone where tension is theorized to be highest in this sort of impact (Turner, 2005). In imaging dynamic phenomena, higher image resolution was found to be a trade-off with collection rate, the implications of which must be considered in future applications.

When synchronized with bead and screw displacement data, video captured using the high-speed x-ray system exhibited metal bead position changes of less than 0.1 mm between still frames. Larger displacements of the more superior bead compared to other tracked entities confirms elastic deformation of the entire femur, preventing classification of the specimen as a rigid body in analysis. This behavior is not unexpected for such materials (composite foams) when subjected to forces below their yield point. The fracture induced in Phase 3 was recognized as a clinically relevant fracture observed when the lateral cortex screw hole is placed below the level of the lesser trochanter. The hole made by the screw through the cortical bone as the initiation site of the fracture makes sense due to the increased stress localized to this region. Furthermore, other relevant work has demonstrated proximal femur fracture initiating in the sideways fall at the location of much smaller perforations of the cortical bone (Bahaloo et al., 2017).

Previous work quantified the bead tracking precision and accuracy of the x-ray system used in this study to be 0.025 ± 0.01 mm and 0.019 ± 0.017 mm, respectively (Lucas et al., 2018). Lucas reported an average resolution of 0.125 ± 0.001 mm/pixel, whereas the resolution at an instance of our n=1 test was found to be 0.15 mm/pixel. Our methods set the camera resolution at a slightly smaller window than previous approaches (800 x 768 pixels compared to 800 x 800) which could contribute to this difference. Bead tracking accuracy was not calculated in this work. However, our calculations showed the specimen to move in free fall at an average vertical velocity of rate of 2.86 ± .08 m/s, which is in the range of the target velocity of the fall simulator (Fleps et al., 2018). This is encouraging with respect to the ability to accurately track metal beads and orthopedic hardware in future tests.

The demonstrated feasibility and initial outcomes of these pilot tests are promising with respect to application of this imaging method to the fall simulator protocol and specimen preparation proposed by Fleps et al. It is well documented that rate of loading greatly informs fracture load and behavior of bone (Courtney et al., 2007). Furthermore, both the effective stiffness of the pelvis (Laing et al, 2010) and soft tissue over the greater trochanter (Bouxsein et al., 2007) affect the load experienced by the femur in a sideways fall. Despite offering valuable information on fracture pathomechanics on the micro- and nano- scale, previous approaches capturing fracture propagation with x-ray have neglected to account for these variables in either specimen preparation (Ma et al., 2020) or applied loading rate (Martelli et al., 2018). For clinical and biomechanical relevance, it is imperative that data concerning fracture phenomena be collected in as biofidelic of an injury scenario as possible. Additionally, high-speed video analysis is inadequate for capturing fracture occurrence behind soft tissue, especially since some fractures may initiate in the cancellous bone (Bahaloo et al., 2017). The results presented in this proof-of-concept work suggest that we will be able to capture such phenomena in future applications of this novel method.

There are limitations to this work, many inherent to the n=1 sample size used in these phased pilot tests. As it was designed to be a proof-of-concept analysis, our study lacked statistical power to draw meaningful conclusions on fracture behavior during impact. However, this was not the goal of our research and outside the scope of what we sought to achieve. The x-ray data collected was distorted and uncalibrated beyond scaling 2D data to an object of known size in ImageJ software, and measured displacement was in a single plane and did not track potential 3-dimensional motion. The basic ability to capture video of fracture behavior as it occurs was deemed sufficient to determine basic feasibility of this approach, and we predict that undistortion and calibration will only improve the quality of future visual data. Despite knowing the collection rate at which the video camera recorded the image intensifier screen, the effective capture rate of the system as a whole remains unknown. Detailed impact phenomena such as smaller fracture or micromotions may occur at too high of a speed to be recorded by our system.

The injury biomechanics of trauma experienced by humans implanted with orthopedic hardware has been relatively unexplored in the literature to date. Fixation of fracture and other skeletal injury using metal implants remains a popular method in clinical practice and we anticipate increased interest in this field as periprosthetic injury continues to rise (Della Rocca et al., 2011). To the authors' knowledge, studying the relative motion of implants and bone on a macro scale during an injurious event has not yet been pursued. Observing the interactions between bone and implant are key to understanding why and how periprosthetic fracture occurs, and how it can be prevented. High-speed video alone to analyze impact tests does not allow for a comprehensive understanding of the essential role that the implant plays in periprosthetic fracture propagation, as it is fully internal to the bone. The use of high-speed x-ray allows for motion data to be collected during the course of the impact, rather than position data typically collected in pre- and post-impact scans. To this end, the future applications of the pilot tests presented in this work are encouraging.

CONCLUSIONS

The results of this pilot study demonstrate the ability to observe hip fracture using the high-speed x-ray system with the fall simulator. The presented tool is theorized to offer more robust capabilities than current imaging techniques to observe bone mechanics during realistic impact tests. Obtaining such data could be key to understanding and ultimately preventing hip fractures. In the future, this method will be used to image ex vivo pelvis-femur specimens in a biofidelic soft tissue surrogate. Further, we hope to improve on our methods by adding a second x-ray system to allow for visualization and quantification in three dimensions. Successful integration of a biplanar system would enable a more robust analysis of impact and fracture mechanics.

ACKNOWLEDGEMENTS

The authors would like to thank Vivian Chung and Kurt McInnes for offering their help and knowledge with use of equipment necessary to carry out this project. We would also like to acknowledge the Four-Year Fellowship and UBC Department of Orthopaedics for generously providing the funding to support this work.

REFERENCES

BAHALOO, H., ENNS-BRAY, W.S., FLEPS, I., ARIZA, O., GILCHRIST, S., WIDMER SOYKA, R., GUY, P., PALSSON, H., FERGUSON, S.J., CRIPTON, P.A., HELGASON, B. (2017). On the failure initiation in the proximal human femur under simulated sideways fall. Annals of Biomedical Engineering 34(3), 270-283.

BHATTACHARYYA, T., CHANG, D., MEIGS, J.B., ESTOK, D.M., MALCHAU, H. (2007) Mortality after periprosthetic fracture of the femur. The Journal of Bone and Joint Surgery 89, 2658-2662.

BOUXSEIN, M.L., SZULC, P., MUNOZ, F., THRALL, E., SORNAY-RENDU, E., DELMAS, P.D. (2007). Combination of trochanteric soft tissues to fall force estimates, the factor of risk, and prediction of hip fracture risk. Journal of Bone and Mineral Research 22(6), 825-831.

COOPER, C., COLE, Z.A., HOLROYD, C.R., EARL, S.C., HARVEY, N.C., DENNISON, E.M., MELTON, L.J., CUMMINGS, S.R., KANIS, J.A. (2011). Secular trends in the incidence of hip and other osteoporotic fractures. Osteoporosis International 22, 1277-1288.

COURTNEY, A.C., WACHTEL, E.F., MYERS, E.R., HAYES, W.C. (1995). Age-related reductions in the strength of the femur tested in a fall-loading configuration. The Journal of Bone and Joint Surgery 77-A(3), 387-395.

CRAIG, M., BIR, C., VIANO, D., TASHMAN., S. (2008). Biomechanical response of the human mandible to impacts of the chin. Journal of Biomechanics 41, 2972-2980.

DE BAKKER, P.M., MANSKE, S.L., EBACHER, V., OXLAND, T.R., CRIPTON, P.A., GUY, P. (2009) During sideways falls proximal femur fractures initiate in the superolateral cortex: Evidence from high-speed video of simulated fractures. Journal of Biomechanics 42, 1917-1925.

DELLA ROCCA, G.J., LEUNG, K.S., PAPE, H. (2011). Periprosthetic fractures: Epidemiology and future projections. Journal of Orthopedic Trauma 25(6), S66-S70.

DIOTALEVI L., WAGNAC, E., LAURENT., H., PETIT, Y. (2020). In vitro assessment of the role of the nucleus pulposus mechanism of vertebral body fracture under dynamic compressive loading using high-speed cineradiography. Annual International Conference of the IEEE Engineering in Medicine and Biology Society, July, 4717-4720.

FLEPS, I., VUILLE, M., MELNYK, A., FERGUSON, S.J., GUY, P., HELGASON, B., CRIPTON, P.A. (2018). A novel sideways fall simulator to study hip fractures ex vivo. PLOS ONE 13:e0201096.

GUTOWSKI C., DARVISH K., LISS, F.E., ILYAS, A.M., JONES, C.M. (2015). Use of high-speed x ray and video to analyze distal radius fracture pathomechanics. Thomas Jefferson University Department of Orthopaedic Surgery Faculty Papers, Paper 80.

HALEEM, S., LUTCHMAN, L., MAYAHI, R., GRICE, J.E., PARKER, M.J. (2008). Mortality following hip fracture: Trends and geographical variations over the last 40 years. Injury 30, 1157-1163.

KNÖRLEIN, B.J., BAIER, D.B., GATESY, S.M., LAURENCE-CHASEN, J.D., AND BRAINERD, E.L. (2016). Validation of XMALab software for marker-based XROMM. Journal of Experimental Biology 219, 3701-3711.

LAING, A.C., ROBINOVITCH, S.N. (2010). Characterizing the effective stiffness of the pelvis during sideways falls on the hip. Journal of Biomechanics 43, 1898-1904.

LUCAS, E., WHYTE, T., LIU, J., RUSSELL, CL., TETZLAFF, W., CRIPTON, P.A. (2018). High-speed fluoroscopy to measure dynamic spinal cord deformation in an in vivo rat model. Journal of Neurotrauma 35(21), 2572-2580.

MA, S., GOH, E.L., TAY, T., WILES, C.C., BOUGHTON, O., CHURCHWELL, J.H., WU, Y., KARUNARATNE, A., BHATTACHARYA, R., TERRILL, N., COBB, J.P., HANSEN, U., ABEL, R.L. (2020). Nanoscale mechanisms in age-related hip-fractures. Nature Scientific Reports 10:14208.

MARTELLI, S., PERILLI, E. Time-elapsed synchrotron-light microstructural imaging of femoral neck fracture. (2018). Journal of the Mechanical Behavior of Biomedical Materials 84, 265-272.

PARKKARI, J., KANNUS, P., PALVANEN, M., NATRI, A., VAINIO, J., AHO, H., VUORI, I., JÄRVINEN, M. (1999) Majority of hip fractures occur as a result of a fall and impact on the greater trochanter of the femur: A prospective controlled hip fracture study with 206 consecutive patients. Calcified Tissue International 65, 183-187.

THORHAUER, E. (2020). Calibration and optimization of a biplane fluoroscopy system for quantifying foot and ankle biomechanics. University of Washington, Thesis (Master's).

TURNER, C.H. (2005). The biomechanics of hip fracture. The Lancet 366, 98-99.

U.S. CONGRESS OFFICE OF TECHNOLOGY ASSESSMENT (1994). Hip fracture outcomes in people age 50 and over – background paper. US Government Printing Office, OTA-BP-H-120.

WHYTE, T., LIU, J., CHUNG, V., MCERLANE, S.A., ABEBE, Z.A., MCINNES K.A., WELLINGTON, C.L., CRIPTON, P.A. (2019). Technique and preliminary findings for in vivo quantification of brain motion during injurious head impacts. Journal of Biomechanics 95:109279.